

Article

Characterizing Bushfire Occurrences over Jamaica Using the MODIS C6 Fire Archive 2001–2019

Candice S. Charlton , Tannecia S. Stephenson , Michael A. Taylor and Christina A. Douglas

Department of Physics, The University of the West Indies, Kingston 07 JMAAW15, Jamaica; michael.taylor@uwimona.edu.jm (M.A.T.); christina.douglas02@uwimona.edu.jm (C.A.D.)

* Correspondence: candice.charlton02@uwimona.edu.jm (C.S.C.); tannecia.stephenson02@uwimona.edu.jm (T.S.S.)

Abstract: There is an increasing need to develop bushfire monitoring and early warning systems for Jamaica and the Caribbean. However, there are few studies that examine fire variability for the region. In this study the MODIS C6 Fire Archive for 2001–2019 is used to characterize bushfire frequencies across Jamaica and to relate the variability to large-scale climate. Using additive mixed model and backward linear regression, the MODIS represents 80% and 73% of the local Jamaica Fire Brigade (JFB) data variability for 2010–2015, respectively. However, the MODIS values are smaller by a factor of approximately 30. The MODIS climatology over Jamaica reveals a primary peak in March and a secondary maximum in July, coinciding with months of minimum rainfall. A significant positive linear trend is observed for July–August bushfire events over 2001–2019 and represents 29% of the season’s variability. Trends in all-island totals in other seasons or annually were not statistically significant. However, positive annual trends in Zone 2 (eastern Jamaica) are statistically significant and may support an indication that a drying trend is evolving over the east. Significant 5-year and 3.5-year periodicities are also evident for April–June and September–November variability, respectively. Southern Jamaica and particularly the parish of Clarendon, known for its climatological dryness, show the greatest fire frequencies. The study provides evidence of linkages between fire occurrences over Jamaica and oceanic and atmospheric variability over the Atlantic and Pacific. For example, all-island totals show relatively strong association with the Atlantic Multidecadal Oscillation. The study suggests that development of an early warning system for bushfire frequency that includes climate indices is possible and shows strong potential for fire predictions.

Keywords: Caribbean; bushfires; MODIS; wavelet; climate; Jamaica; fire variability; SIDs



Citation: Charlton, C.S.; Stephenson, T.S.; Taylor, M.A.; Douglas, C.A. Characterizing Bushfire Occurrences over Jamaica Using the MODIS C6 Fire Archive 2001–2019. *Atmosphere* **2021**, *12*, 390. <https://doi.org/10.3390/atmos12030390>

Academic Editor: Luis Gimeno

Received: 20 February 2021

Accepted: 11 March 2021

Published: 17 March 2021

Publisher’s Note: MDPI stays neutral with regard to jurisdictional claims in published maps and institutional affiliations.



Copyright: © 2021 by the authors. Licensee MDPI, Basel, Switzerland. This article is an open access article distributed under the terms and conditions of the Creative Commons Attribution (CC BY) license (<https://creativecommons.org/licenses/by/4.0/>).

1. Introduction

Bushfires are a growing concern for small island developing states (SIDs) like Jamaica and other Caribbean islands and their occurrence each year has immense social, economic and environmental impacts. From 2016 to 2019, the number of bushfires across Jamaica increased from 3716 to 5838 [1]. Fire activity may be triggered or exacerbated by the prevailing climate conditions with other important influences including fuels, ignition agents and human activity [2–4]. Some climate conditions promoting fire activity include rainfall deficits, extreme temperatures, heat waves and dry windy conditions that may occur in relation to large-scale modes such as the El Niño South Oscillation (ENSO). These promote the availability of fuels for fire as well as mechanisms for fire spread. A summary of some major fire events in Jamaica for 2014–2019 including costs and associated prevailing climate is shown in Table 1. While the impacts of fire events are apparently increasing within the Caribbean, there are few studies and reports that examine fire variability for this region (e.g., [5–8]). Robbins [7] indicates that the Caribbean lags areas in the United States in terms of fire prediction, monitoring, education, prevention, and analysis of the effects of fire on ecosystems and society.

Table 1. Some bushfire events in Jamaica between 2014–2019 as reported by The Gleaner, the Jamaica Observer and Jamaica Information Service. The total area burned, estimated loss at time of reporting in Jamaica Dollars and the background climate event are also indicated.

Year	Location	Total Area Burned	Estimated Loss	Climate Event
2014	Bull Bay, St Thomas to Mavis Bank, St Andrew	200 Acres	Approximately JMD 136 Million	Meteorological Drought (MD) Source: CIMH Caribbean Drought Bulletin Vol 1 Issue 6 November 2014
2015	St Thomas Blue Mountain (Mavis Bank)	>247 Acres 500 Acres	Approximately JMD 146 Million Approximately JMD 300 Million	Very Strong El Niño Source: http://www.bom.gov.au/climate/enso/enlist/ (accessed on 18 August 2020)
2016	Bull Bay, St Thomas Mount Charles, St Andrew Craig Hill, St Andrew	-	-	-
2017	Roselle, St Thomas Pangully-Glengoffe, Cassava River St Catherine	>100 Acres	-	-
2019	Flagaman, St Elizabeth	>200 Acres	JMD 45 Million	El Niño Source: https://origin.cpc.ncep.noaa.gov/products/analysis_monitoring/ensostuff/ONI_v5.php (accessed on 18 August 2010)

Linkages between bushfire characteristics (e.g., occurrence, ignition, intensity, burned area and pattern, potential spread) and climate variability and extremes have been examined globally including for North America [9], Australia [10], Portugal [11], Alaska [12], Mediterranean [13] and Hawaii [14]. These studies link wildfire frequency and area burned to droughts, heat waves, climate modes such as the ENSO and anthropogenic influences (Table 2). These studies are executed using land-based observations and satellite products such as the NASA Moderate Resolution Imaging Spectroradiometer (MODIS) fire archives to represent fire activity data. The MODIS has presented an attractive option for fire studies since ground-based observations (e.g., Burned Area) are commonly affected by periods of unavailable or poor-quality data [15,16]; difficulties in the estimations of Burned Area from field observations [17,18] and protocol changes over time [19].

In this research the following questions are explored: How representative is the MODIS C6 fire archive of bushfire variability in Jamaica? What are some temporal and spatial characteristics of bushfire occurrences across the island? What are some local and large-scale climate features or phenomena that may be associated with bushfire variability across the island? The importance of this study, then, lies firstly in its contribution to the limited body of knowledge on bushfire variability and its linkages to climate in the Caribbean and SIDS in general. The work is critical as some of the hotter and drier extremes that may promote increased bushfire variability are already evident in the Caribbean. An analysis of weather and climate extremes for the Caribbean over 1961–2010 reveal increases in the annual means of daily minimum ($0.28\text{ }^{\circ}\text{C decade}^{-1}$) and maximum temperatures ($0.1\text{ }^{\circ}\text{C decade}^{-1}$), increased frequencies of warm days, warm nights and extreme high temperatures and decreases in the frequency of cool days, cool nights and extreme low temperatures. Small but significant positive trends were found in annual total precipitation, daily intensity, maximum number of consecutive dry days and heavy rainfall events particularly during the latter period 1986–2010 [20,21]. Other investigations have indicated an increase in the occurrence of extreme events including droughts [22].

The climate conditions that may exacerbate increased bushfire frequency are also expected to continue and intensify towards the middle to end of century through increases in warm day and warm night occurrences and decreases in cool days and cool nights [23–26]. A future trend of increased daily rainfall intensity and a decrease in the proportion of total rainfall from heavy rainfall events were also noted in these studies. For example, by the end of the century, the Caribbean is projected to be 1.08 to 3.58 °C warmer [24,27,28], with 95% of all days and nights considered “hot” (i.e., exceeding the 90th percentile of current temperatures; [23]). Annual rainfall totals are projected to decrease by up to 30% with the most pronounced drying during the Caribbean wet season from May and October [27–29]. This latter projected drying would have serious implications for an extension of the “fire season” within the Caribbean.

Jamaica, through its meteorological service and the Jamaica Fire Brigade, is currently undertaking efforts to develop a Bush Fire Warning Index to track, manage and record bushfires. This effort is funded under the African Caribbean Pacific-European Union-Caribbean Development Bank Natural Disaster Risk Management (ACP-EU-CDB NDRM) program. The Index will act as a predictive tool to encourage pre-emptive action and prevent fires from destroying forests, farms and the livelihoods of families across the country. This is one of many efforts within Caribbean SIDS that recognizes the perceived increasing impact of bushfires on Caribbean lives and livelihoods.

This study, therefore, is also significant as it provides baseline information in support of this effort, through the quantification of fire, frequency and variability across Jamaica.

Data and methodology for characterizing fire activity in Jamaica are presented in Section 2. Section 3 describes bushfire spatial and temporal characteristics and investigates linkages with several large-scale climate phenomena that are important to climate variability within the Caribbean and some local climate features important to Jamaica. Section 4 discusses the results and implications, including for the wider Caribbean.

Table 2. Fire characteristics and their relation to climate for some regions. Data sources and references are also shown.

Region	Fire Data Source/Fire Indices	Observations in Relation to Climate	References
Alaska	Alaska Fire Service Data (1955–2009)	<ul style="list-style-type: none"> • Above normal summer temperatures linked with increased convection amounts, resulting in higher number of lightning strikes. Dry conditions in adjacent areas facilitate the spread of wildfires started by the lightning. • Correlation between the Palmer Drought Severity Index and Canada Drought Code against number of wildfires and area burnt yielded relatively low values with some statistically significant. 	[12]
Australia	Daily meteorological data (1973–2017) including maximum temperature ($^{\circ}\text{C}$), relative humidity (%), wind speed (kmh^{-1}); derived drought factor calculated using the Keetch Byram Drought Index (KBDI) for calculation of McArthur Forest Fire Danger Index (FFDI)	<ul style="list-style-type: none"> • El Niño Southern Oscillation (ENSO) is the main driver for interannual variability of fire weather, as defined by FFDI. • In New South Wales, particularly along the central coast, negative Southern Annular Mode (SAM) is a primary influence for elevated fire weather in late-winter and spring. In southeast Australia, the El Niño-like impact is exacerbated when positive Indian Ocean Dipole (IOD) conditions are simultaneously observed. 	[10]
Hawai'i	<p>Three local repositories of territorial and state reports of area burnt for 1901–2004.</p> <p>Fire occurrences from Hawai'i Wildfire Management Organization (1967–2003).</p> <p>Wildfire conditions obtained from HWMO records (2005–2011) for which complete records from all agencies are available</p>	<ul style="list-style-type: none"> • Ignitions occurred year-round with peaks in the summer (June, July, August) and winter months (January, December). • Area burned showed a large increase during the summer months. 	[14]
Mediterranean	<p>Four state-of-the-art satellite fire products related to Moderate Resolution Imaging Spectroradiometer (MODIS) (2001–2016) and fourth generation of the Global Fire Emissions Database (1995–2016).</p> <p>Gridded, ground-based European Forest Fire Information System (EFFIS) dataset (1985–2015)</p>	<ul style="list-style-type: none"> • Burned area showed strongest periodicity in the summer months across datasets. 	[13]

Table 2. Cont.

Region	Fire Data Source/Fire Indices	Observations in Relation to Climate	References
North America	Palmer Drought Severity Index; Standard Precipitation Index; KBDI; Fosberg fire weather index (FFWI).	<ul style="list-style-type: none"> • Drought increases probability of fire occurrence in forest ecosystems, but other biotic and abiotic disturbances and stressors interact with drought and fire. • Temperature increases are a predisposing factor causing often lethal stresses on forest ecosystems acting both directly through increasingly negative water balances, and extent of disturbances, chiefly fire and insect outbreaks 	[9]
Portugal	Local records	<ul style="list-style-type: none"> • Intra and inter-annual variability in the heat waves characteristics are clearly associated to the spatial-temporal distribution of the extreme wildfires. • Total extreme wildfire days were also heat wave days. • Extreme wildfire had duration completely contained in the duration of a heat wave. • Extreme wildfires occurred during and in the area affected by heat waves. 	[11]

2. Materials and Methods

2.1. Materials

2.1.1. Study Area

Jamaica is the third largest Caribbean island and is divided into fourteen parishes. Walters [30] and Douglas [31] suggest that there are four rainfall zones which they classify as: Interior (zone 1); East (zone 2); West (zone 3) and North and South Coasts (zone 4). See Figure 1. Zones were deduced from the cluster analysis of 129 stations across Jamaica for 1971–2010 to which Young’s Estimation data infilling technique was applied and that were validated against the 1971–2000 mean annual rainfall map produced by the Meteorological Service Jamaica [30]. Douglas [31] confirmed the 4 zones using cluster analysis of 23 stations across Jamaica chosen for their length and completeness over 1971–2010. Zones 1, 3 and 4 show bimodal patterns with an early season peaking in May and late season peaking in September with a mid-summer minimum in July [31]. The bimodality is very similar to the double peak pattern noted across islands in the main Caribbean [32,33]. The zones are however differentiated by their seasonal and annual totals. In contrast, zone 2 in the east shows a different climatology, recording its highest rainfall in November and a secondary peak in April–May. This zone also has the highest rainfall totals of all zones [30,31].

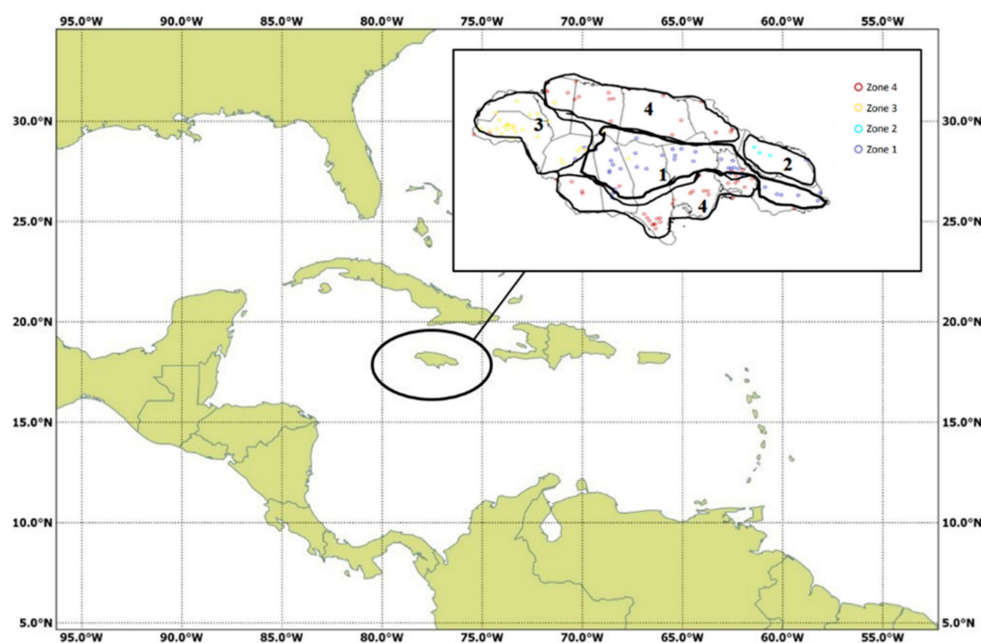


Figure 1. Map of the Caribbean. Inset diagram adapted from State of the Jamaican Climate 2015 showing a map of Jamaica with the approximate bounds for the four rainfall zones.

2.1.2. Fire and Climate Data

Fire occurrence data are obtained from records compiled by the Jamaica Fire Brigade (JFB) over 2010–2015 and from the NASA MODIS C6 fire archives over 2001–2019. The fire data include both human induced and natural fires across the rainfall zones as no differentiation was made in the archives. The JFB data is a monthly compilation of bushfire occurrences across the island that were reported to the JFB and that required their response (even if no intervention). The dataset includes fire locations to the nearest street. The NASA MODIS active fire archive [34] is a global dataset that has a spatial resolution of 1 km and daily data over Jamaica are extracted for 2001–2019. MODIS is an optical sensor on board the Terra and Aqua satellites that were launched on 18 December 1999 and 4 May 2002, respectively. Terra travels on a descending path (north to south, crossing the equator in the morning, while Aqua travels on an ascending path (south to north), crossing the equator in the afternoon. Correspondingly on the other side of their orbit Terra travels an ascending path (south to north), crossing the equator in the afternoon, while Aqua travels

a descending path (north to south), crossing the equator in the morning. This allows for the collection of the entire surface of Earth every 1 to 2 days. The MODIS sensor collects data in 36 spectral bands with a swath of 2330 km (across track) by 10 km (along track) and has a spatial resolution from 0.25 to 1 km dependent on the band. Bands 1 and 2 (red and infrared) offer a spatial resolution of 0.25 km, bands 3 to 7 offer a spatial resolution of 0.50 km, and the remaining bands 8–36 collect imagery at 1 km spatial resolution. The MODIS active fire products were developed using active fire detection algorithms based on heritage algorithms previously developed for Advanced Very High-Resolution Radiometer and Tropical Rainfall Measuring Mission–Visible and Infrared Scanner [7,35].

The climate indices used in this study and their sources are summarized in Table 3. The indices include all island monthly rainfall, Niño3 sea surface temperature anomalies (SSTA), Tropical North Atlantic (TNA) SSTA, Tropical South Atlantic (TSA) SSTA, Caribbean low level winds (LLW) anomalies, North Atlantic Oscillation (NAO), Atlantic Multidecadal Oscillation (AMO) and Pacific Decadal Oscillation (PDO). The climate indices have been identified in previous studies as important to climate variability over the Caribbean [20,36–38].

Table 3. Some climate indices used in correlation analyses. Anomalies are calculated relative to 2001–2019.

Climate Indices	Definition	Reference
TNA	Area average of monthly sea surface temperature (SST) anomalies over 5.5° N–23.5° N and 15° W–57.5° W. Data: HadISST and NOAA OI 1° × 1°. Source: https://psl.noaa.gov/data/correlation/tna.data (accessed on 10 February 2020)	[36]
TSA	Area average of monthly SST anomalies over 0°–20° S and 10° E–30° W. Data: HadISST and NOAA OI 1° × 1°. Source: https://psl.noaa.gov/data/correlation/tsa.data (accessed on 10 February 2020)	[36]
NINO 3.0	Area average of monthly SST anomalies over 5° N–5° S and 150° W–90° W. Monthly ERSSTv5 are used to create index. Source: https://www.cpc.ncep.noaa.gov/data/indices/ersst5.nino.mth.81-10.ascii (accessed on 10 February 2020)	[39,40]
Low level winds	Area average of monthly zonal wind anomalies over 70°–80° W, 12.5°–17.5° N. Data: NCEP/NCAR Reanalysis 2.5° × 2.5°	[41,42]
NAO	The index is obtained by projecting the NAO loading pattern, 1st mode of the Rotated Empirical Orthogonal Function, to the daily anomaly 500 mb height field over 0°–90° N. Source: https://www.cpc.ncep.noaa.gov/data/teledoc/nao.shtml (accessed on 10 February 2020)	[43]
AMO	An area weighted average of anomalies calculated over the North Atlantic Ocean (0° to 70° N) on the Kaplan SST dataset (5° × 5°) and the 1951–1980 interpolated NOAA ERSST V2 SST climatology was added back in. Data is unsmoothed and not detrended. Source: https://www.esrl.noaa.gov/psd/data/timeseries/AMO/ (accessed on 25 March 2020)	[44]
PDO	Standardised values of the PDO index are derived as the leading Principal Component of monthly sea surface temperature anomalies in the North Pacific Ocean (poleward of 20° N). Source: http://research.jisao.washington.edu/pdo/PDO.latest.txt (accessed on 25 March 2020)	[45,46]

2.2. Methods

2.2.1. Validation of the MODIS Data

The JFB dataset is compared with the MODIS to determine the representativeness of the MODIS data given the limited 6-year time span of the JFB data. An all island monthly bushfire frequency timeseries is calculated for each dataset using total fire occurrences per month and is used for the following analyses. Firstly, the correlation coefficient between the JFB and MODIS timeseries is calculated over the 2010–2015 period and the statistical significance is determined. The climatologies of the JFB and the MODIS are calculated over a common 2010–2015 period. The climatology for the MODIS over 2001–2019 is also calculated. The data are also compared with the 2010–2015 rainfall and maximum temperature climatology. The raw monthly timeseries of both fire datasets over 2010–2015 are also plotted. Finally, a Generalized additive mixed model (GAMM) was applied to explore the strength of the relationship between the two fire timeseries. The model indicates how well the MODIS (variable x) is able to predict for the JFB (variable y). The GAMM generally uses cross-validation and includes both spatial and temporal correlations, as well as multiple homogeneity tests [47]. The model explored a direct linear relationship between the indices as well as a spline smoothed random effects relationship. The skill of the model is indicated using Spearman and Pearson Correlations with statistical significance given by p value and F -value.

2.2.2. Characterizing Temporal and Spatial Variability

Average monthly fire occurrences on annual and seasonal timescales are calculated for 2001–2019. Seasons examined are December to March (DJFM), April to June (AMJ), July to August (JA) and September to November (SON) similar to seasons used by CSGM [48]. Seasons are chosen to coincide with Jamaica's wet seasons (AMJ and SON) and dry seasons (DJFM and JA). Trend values and statistical significance are determined using the Mann-Kendall Test [49–51] and Sen's Slope [52]. The Mann-Kendall Test is used to determine whether a timeseries has a monotonic upward and downward trend at a 0.05 alpha level. The test does not require the data to be normally distributed or linear but that there is no autocorrelation. This latter condition however is likely not satisfied in bushfire frequency data given that, for example the atmospheric conditions influencing bushfire variability have some autocorrelation. The Sen's slope is used to determine the magnitude of the trend in a univariate timeseries. The technique does not require any probability distribution. The variability explained is determined using linear regression analyses.

Secondly, annual and seasonal fire frequency anomalies for 2001–2019 are calculated. Annual anomalies for the JFB data for 2010–2015 are also calculated. Annual and seasonal anomalies are further disaggregated by rainfall zones and plotted. Wavelet analyses are then applied to the normalized annual and seasonal averages for 2001–2019 as well as to the normalized annual means over each rainfall zone to quantify the periodicities that are observed. Wavelet decomposes the timeseries into time-frequency space and identifies the dominant modes of variability and how these modes vary in time. Wavelet is also an efficient approach to analyse nonstationary signals [53]. The wavelet-transform of a real signal $X(t)$ used to extract time and frequency information from the $X(t)$ climate data with a mother wavelet ψ , is a convolution integral given as

$$W_n(s) = \frac{1}{\sqrt{s}} \int_0^T X(t) \psi^* \left(\frac{t-n}{s} \right) dt, \quad (1)$$

where ψ^* is the complex conjugate of ψ , t is the time, T is the total length of the time series, s is the scale, n is translated position along the t axis and $W_n(s)$ is a wavelet spectrum, a matrix of energy coefficients of the decomposed time series [54].

The distribution of the fire activity over 2001–2019 is plotted over Jamaica with four rainfall zones shown. The interpolated fire activity is also represented by seasons to highlight the seasonality of fire activity over the island spatially.

2.2.3. Exploring Climate Linkages

Annual and seasonal all island timeseries are correlated with the suite of indices in Table 3. The indices are calculated on annual timescales. Concurrent and lag correlations are calculated to identify those phenomena related to fire variability over Jamaica and that may be useful in a predictive scheme. Correlations are also calculated between the annual and seasonal fire activity timeseries and low pass filtered AMO, NAO and PDO. The AMO, NAO and PDO timeseries were normalized and filtered using a Butterworth low pass filter set to a frequency of 0.1 and to an order of 1 to isolate decadal/multidecadal variability. Additional post-processing was undertaken to correct the lagged outcome of the filtered timeseries [31]. Correlations are also calculated with respect to local mean temperature and precipitation. The significance of correlation coefficients at the 0.05 p-value significance level is tested.

To further investigate climate linkages, plots of sea surface temperature and wind speed anomalies are created over an Atlantic and Pacific domain (0° – 180° W, 10° S– 60° N) for composites of four years of strongest above normal fire incidence (2005, 2009, 2010 and 2015) versus four years of strongest below normal incidence (2001, 2002, 2003 and 2016) to identify the dynamical features that may contribute to years of extreme bushfire variability. SSTA are obtained from the $2^{\circ} \times 2^{\circ}$ NOAA Extended Reconstructed Sea Surface Temperature (ERSST) v5 [55]. The latest ERSST estimates have more realistic spatiotemporal variations, better representation of high-latitude SSTs, and ship SST biases are now calculated relative to more accurate buoy measurements, while the global long-term trend remains about the same. Anomalies of zonal wind at 925 mb are obtained from ERA Interim [56]. ERA Interim is a global atmospheric reanalysis from 1979 to 2019 with a spatial resolution of approximately 80 km on 60 levels in the vertical from surface up to 0.1 hPa. Anomalies are calculated with respect to 2001–2019.

3. Results

3.1. Validating MODIS: Models and Climatology

Figure 2 shows a plot of the monthly fire activity over Jamaica from MODIS and the JFB over their overlapping period 2010–2015. The plot shows that there is strong similarity between the variabilities represented by the datasets. The correlation between the monthly timeseries is 0.86. However, the MODIS underestimates monthly fire frequency by a factor of up to 30 likely due to the restriction of the frequency of the satellite passing the area, the distance and impact of cloud cover. Figure 3 shows the climatology of the datasets over 2010–2015 including the rainfall and maximum temperature climatology over the corresponding period as well as the MODIS 2001–2019. The climatologies are almost identical albeit with the MODIS underestimating mean monthly fire frequencies. Notably the MODIS and JFB displays a primary peak in March and a secondary maximum in July, coinciding with months of minimum monthly rainfall. Minima in fire occurrences are noted for June and October during peaks in the rainy season. Generalized additive mixed model (GAMM) and backward linear regression (BLR) analyses are used to investigate the predictive skill of MODIS in relation to the JFB. The GAMM and BLR suggest that the MODIS represents 80% and 73% of the JFB data variability, respectively. Together these analyses indicate that the MODIS is a suitable representation of the JFB and can be used for investigating fire activity over Jamaica.

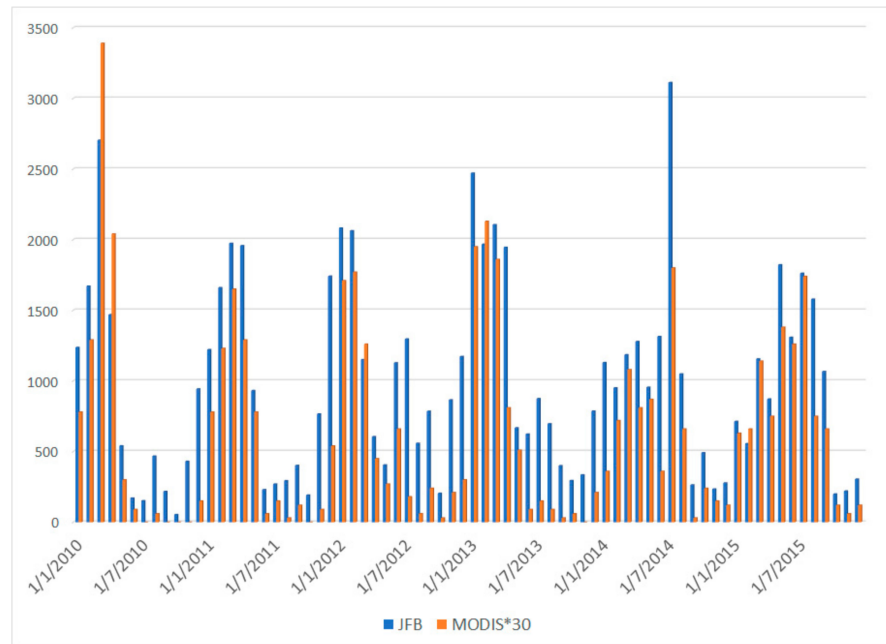
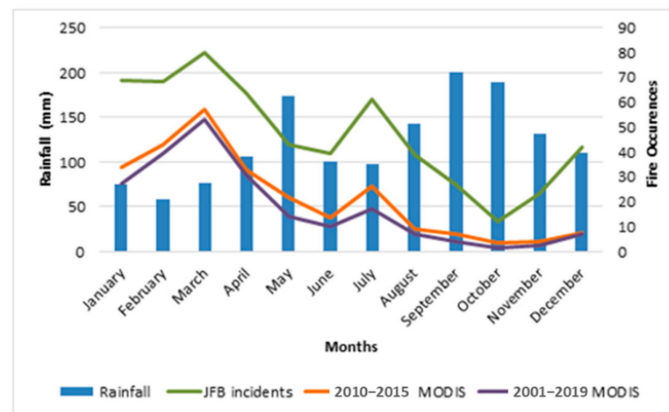
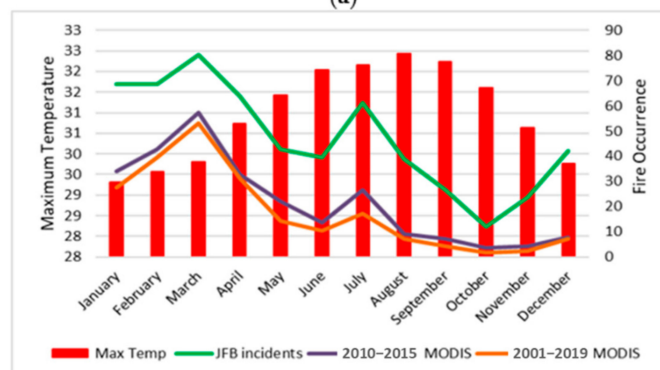


Figure 2. Monthly variations in Jamaica fire frequency data for 2001–2015. The JFB data (blue) and the MODIS data (orange) are shown. The MODIS data is multiplied by a factor of 30 for comparison with the JFB.



(a)



(b)

Figure 3. Climatologies of monthly fire frequency for Jamaica from JFB and MODIS and (a) rainfall and (b) maximum temperature for 2010–2015. Climatology of MODIS fire frequency for 2001–2019 is also shown.

3.2. Temporal and Spatial Variability

Annual and seasonal monthly means are analysed to determine trends in fire activity. Table 4 shows that annually and for all seasons except December–March (DJFM) increases in monthly mean fire frequency are observed. The trend is strongest for July–August (0.9 monthly fires/year) and with the trend representing 30% of the variability. Recall that the MODIS underestimates monthly fire frequencies by a factor of up to 30 suggesting that for July–August (JA) the true trend may be 27 monthly fires/year. The annual trend is 0.3 monthly fires/year. The weakest positive trend is observed in September–November (0.1 monthly fires/year) which explains 9% of the variability. December–March shows negative trend values of 0.5 monthly fires/year which represents 2%. Trends in annual totals by zones are positive except for zone 3 (western Jamaica) where a weak negative near zero trend is observed (Table 5). Trends are strongest for zone 2 (eastern Jamaica) (0.1 monthly fires/year) and zone 4 (northern and southern Jamaica) (0.2 monthly fires/year) explaining 29% and 11%, respectively.

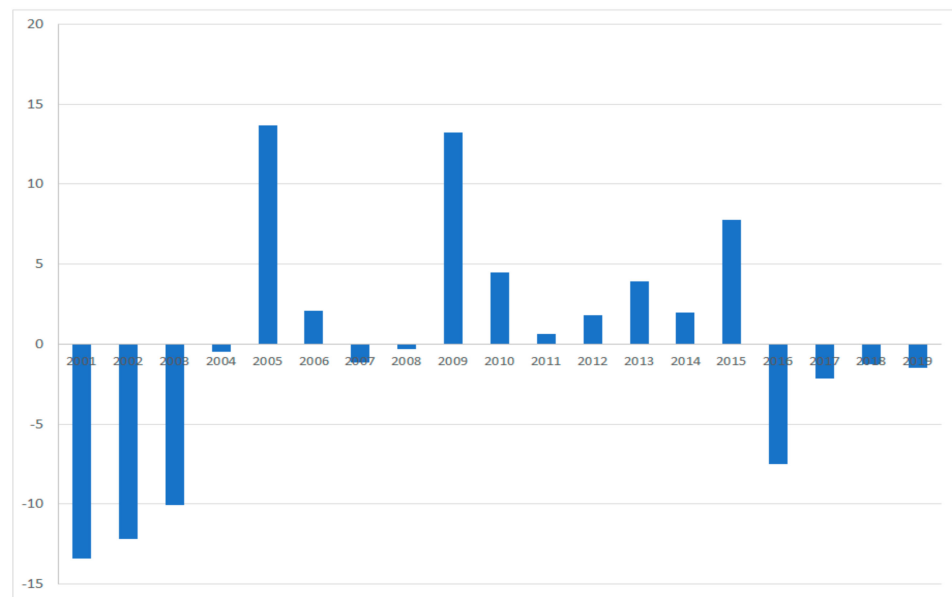
Table 4. Trend values for the all-island fire frequency monthly means calculated annually and for each season December–March, April–June, July–August, and September–November. Values in bold are significant at the 95% level. R^2 is the coefficient of determination and represents the proportion of variance explained by the trend.

Periods	Trend in Monthly Mean (per year)	R^2
Annual	0.3	0.06
DJFM	−0.6	0.02
AMJ	0.4	0.09
JA	0.9	0.30
SON	0.1	0.09

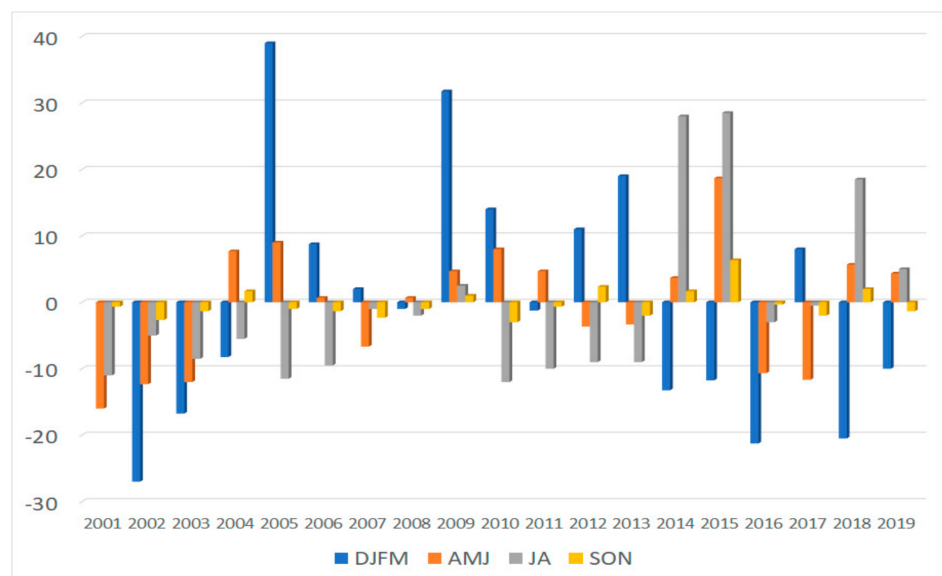
Table 5. Trends in monthly means per year per zones. Values in bold are significant at the 95% level. R^2 is the coefficient of determination and represents the proportion of variance explained by the trend.

Zones	Location	Trend in Monthly Mean (per year)	R^2
1	Interior	0.6	0.03
2	East	0.1	0.29
3	West	0	0
4	North and South	0.2	0.11

Figure 4 shows the annual and seasonal bushfire frequency anomalies for 2001–2019. Interestingly cycles of above normal and below normal monthly fire activity emerge. Annual total fire frequency appears to exhibit a 10-year positive phase switching to its latest negative phase in 2016 (Figure 4a). DJFM appears to show a 9-year positive phase in 2005–2013 with negative phases 2001–2004 and again since 2014 (Figure 4b). A secondary cycle with a smaller periodicity is also observed. AMJ shows fire variability that exhibits a change in phase every 2–3 years. JA exhibits a 13-year negative fire activity phase between 2001–2013, with largely positive values since 2014. SON variability cycle is not as clear.



(a)



(b)

Figure 4. Anomalies of (a) annual means and (b) seasonal means of all island bushfire frequency. Seasons shown are DJFM, AMJ, JA and SON.

In general, there is some evidence of periodicities in the annual and seasonal fire activity and these may in part be related to linkages to climate influences. A longer dataset is required to identify the cycles more definitively. The wavelet analyses on normalized annual and seasonal fire frequency contributes to the evidence that there are periodicities in fire occurrence over Jamaica (Figure 5). The wavelet analysis illustrates regions within the cone of influence where the spectral information is considered reliable. Additionally, the statistical significance of peaks in wavelet power is determined at the 5% significance level by comparing the wavelet power with a red-noise background power spectrum. The results are significant for AMJ and SON where 5 year and 3.5-year cycles, respectively are observed and are within the cone of influence. The AMJ fire variability is particularly strong over 2008–2010. The SON variability shows high intensity peaks in 2010–2015.

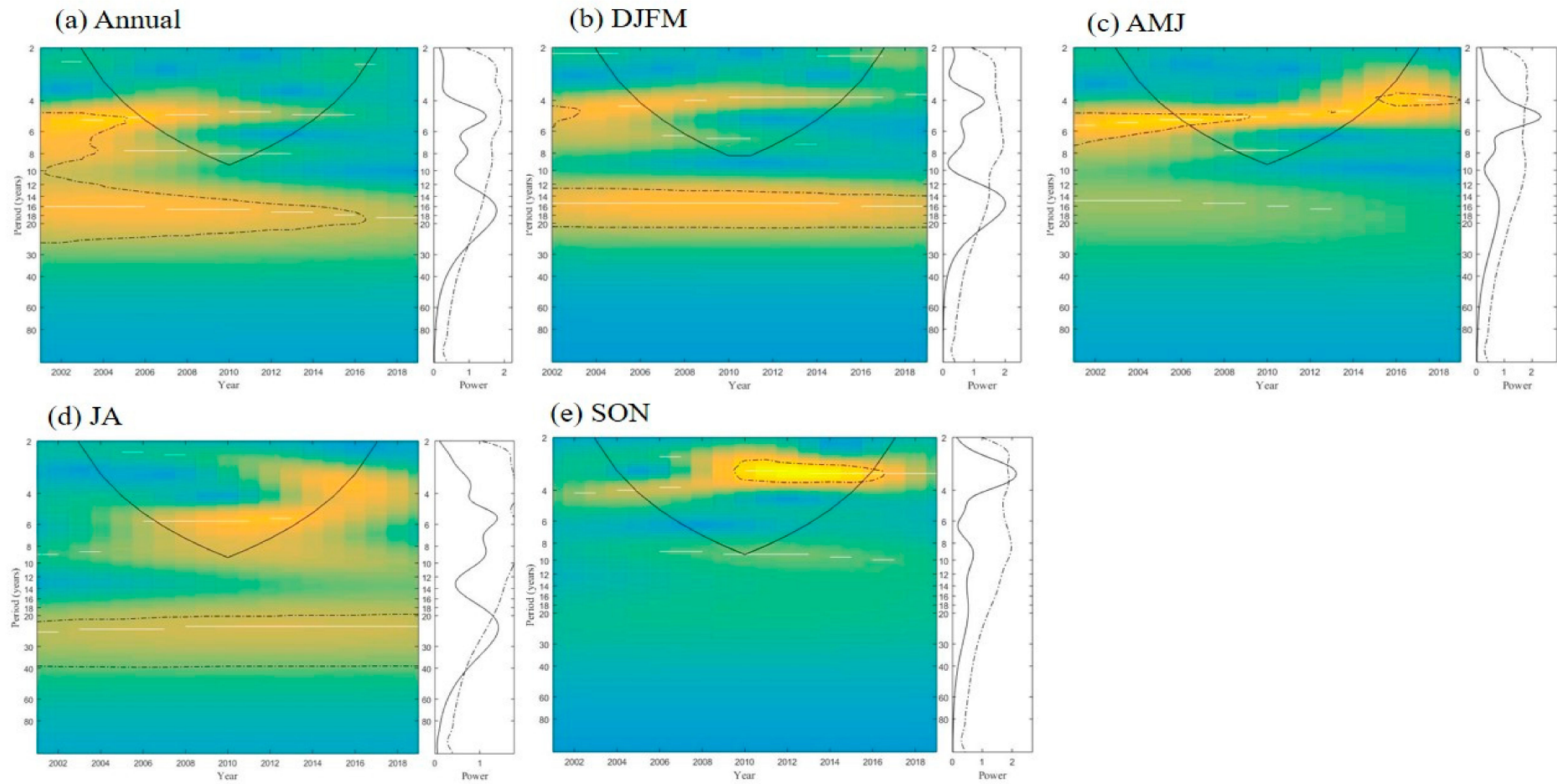


Figure 5. Wavelet analysis of normalized (a) annual and seasonal fire frequency: (b) December–March; (c) April–June; (d) July–August; (e) September–November. The line is the Cone of Influence beyond which the energy is contaminated by the effect of zero padding and the dashed contour line (on spectrum on the right) represents the 95% confidence level of local power relative to a red-noise background.

Periodicities are also evident in annual and seasonal anomalies over each of the four rainfall zones (Figures 6 and 7). Zone 1 (Interior) like DJFM shows a largely positive phase over 2005–2013. Zone 2 (eastern Jamaica) shows very little fire occurrences for 2001–2010 displaying 9 of 11 years with no fires. Fire occurrences show increases and some variability from 2011 onwards. Zone 3 (western Jamaica) displays a 6–7-year cycle over 2001–2019. Zone 4 (northern and southern Jamaica) which accounts for most of the annual fire variability largely mirrors the variability observed for the all island timeseries. An examination of seasonal variability by zone shows most distinct cyclic variability for Zone 4 DJFM where ~4/5 and 9-year cycles are suggested (Figure 7). Zone 2 (eastern Jamaica) and SON for all zones are not shown given that fire frequencies in these instances is minimal. This is expected given that rainfall activity is prevalent for Zone 2 and during SON (the primary rainfall season for much of the island). However, the fire patterns emerging over eastern Jamaica, known for its wetness, may be an indication that a drying trend has been evolving since 2011 over this subregion and has important implications for the island. A wavelet analysis on normalized annual fire frequency by zones reveals a 6-year cycle over Zone 3 (western Jamaica) with high intensity peaks for 2006–2010 (not shown). While other periodicities were identifiable for other zones these lie outside the cone of influence.

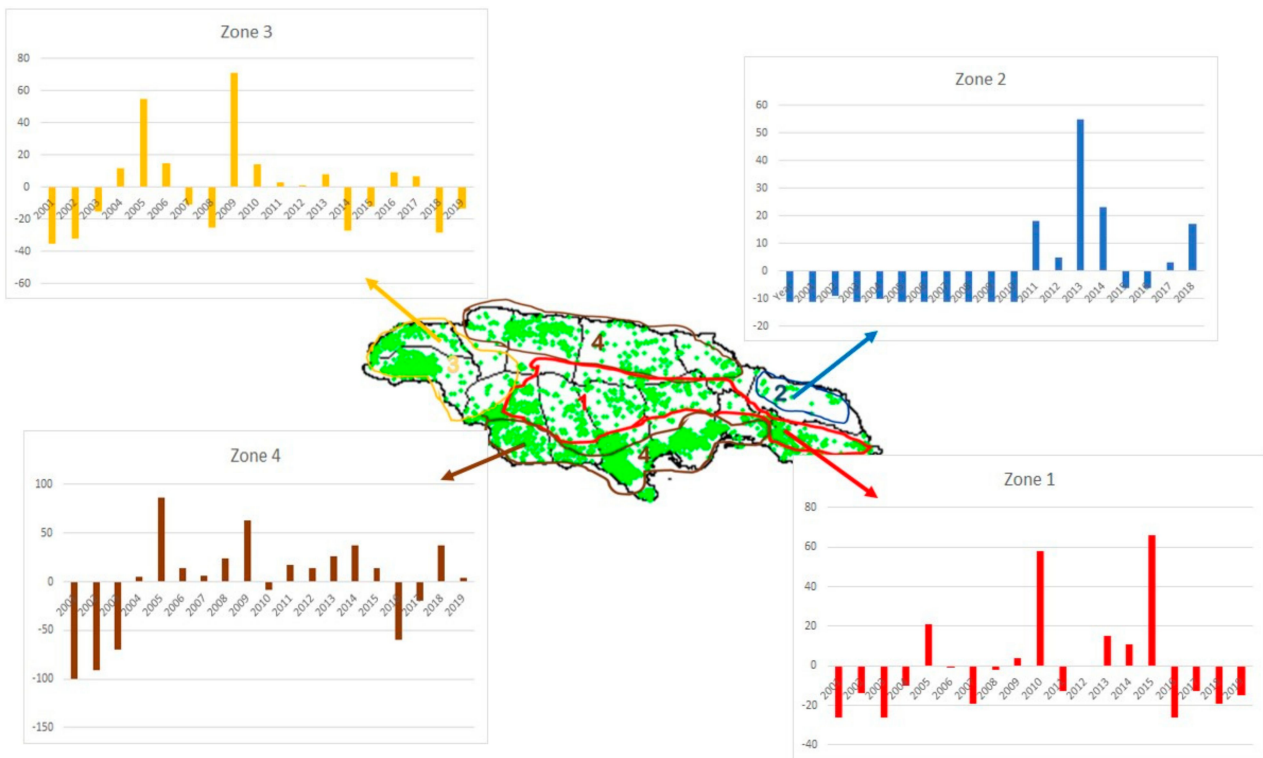


Figure 6. Map showing anomalies of annual fire occurrences for 2001–2019 by zones from the MODIS data. The approximate bounds for the four rainfall zones over Jamaica and the spatial distribution of fires are also shown.

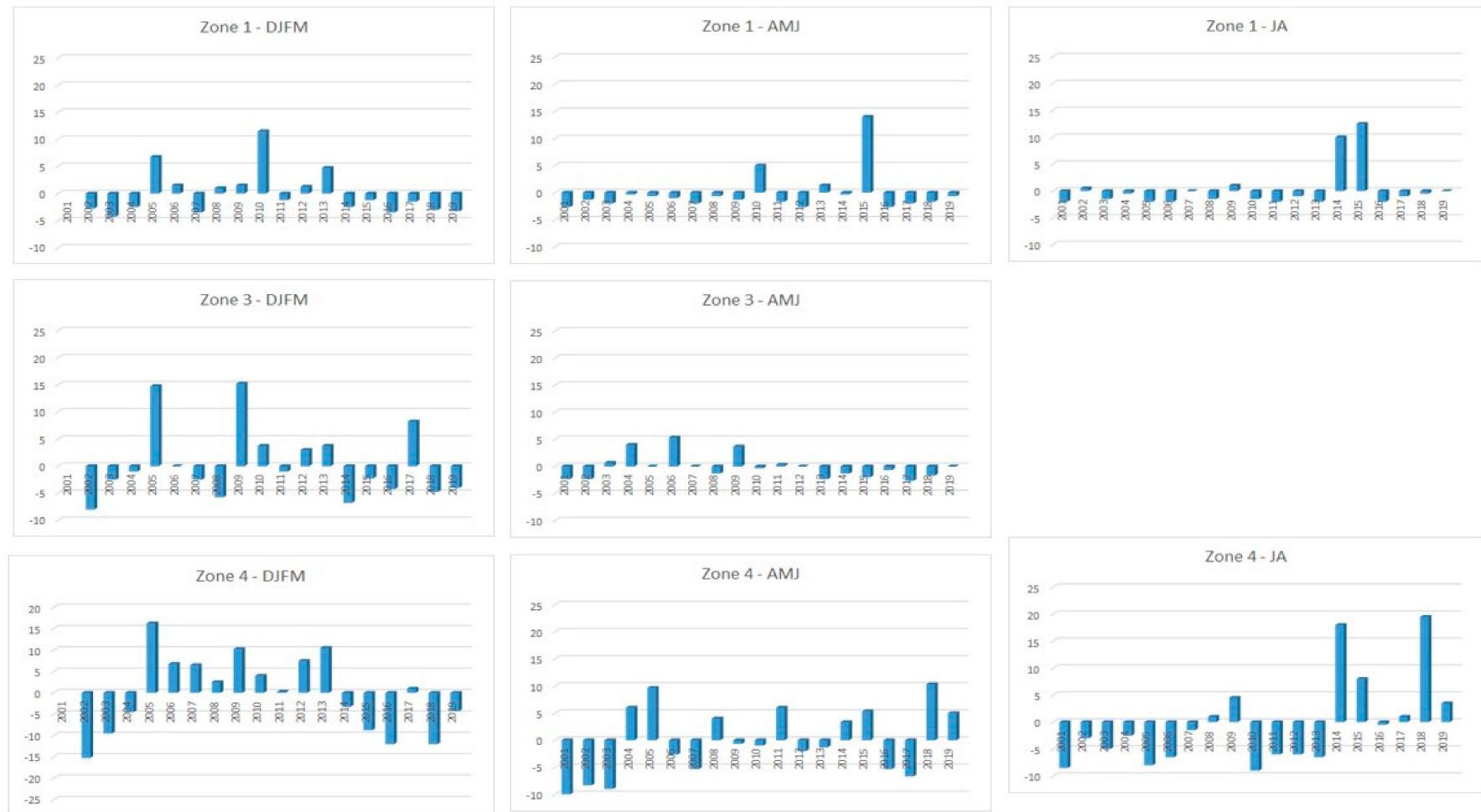


Figure 7. Anomalies of Seasonal fire frequency for zones 1, 3 and 4 for the seasons DJFM, AMJ and JA. Zone 3—JA is omitted since no fire is recorded for most years.

The proliferation of fire activity during December–March is observed spatially in Figure 8. Southern Jamaica shows the greatest intensities during this season and particularly over Clarendon in Southern Jamaica known for its climatological dryness.

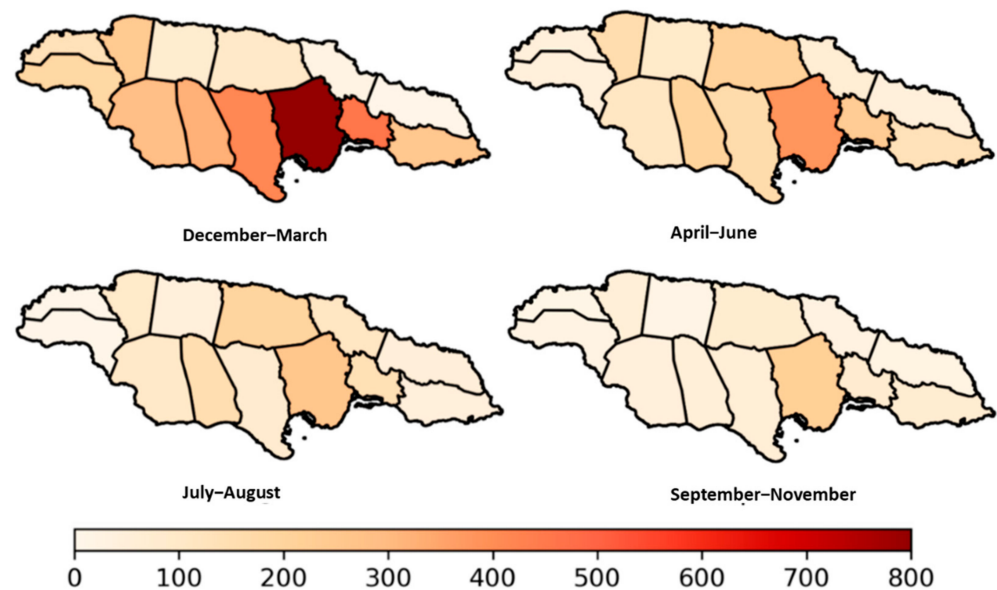


Figure 8. Distribution of Fire Frequencies by seasons for 2010–2015.

3.3. Climate Variability and Fire Frequency Activity

The association between bushfire frequency activity and climate is first explored using correlations. The results are shown in Tables 6 and 7. Some of the key points are noted below:

- Significant correlations are noted in relation to annual and July to November rainfall and temperature. Correlations peak for rainfall in September–November (-0.52) and for temperature in July–August (0.54). Lagged correlations are significant with respect to rainfall (-0.48) and temperature (0.49) for July–August. The low frequency rainfall timeseries showed significant correlations for JA (-0.64) and SON (-0.58).
- Annual and AMJ fire activity exhibits variability similar to the Atlantic Multidecadal Oscillation (0.63 and 0.50 , respectively) and exhibits some association with the Pacific Decadal Oscillation (-0.50) for DJFM. Correlations are also significant with respect to low level winds for DJFM (0.47). These associations are likely through the influence of the AMO and PDO on Jamaica’s rainfall variability.
- JA fire variability correlates significantly with Nino-3 (0.57) and the TNA (-0.59) with a gradient index combining the two indices showing a correlation of 0.68 .
- SON fire variability appears to be related to Nino-3 (0.69), the gradient index (-0.72) and low-level wind in the region of the Caribbean low-level jet (-0.54).

When annual bushfire frequency activity is explored by zone, Zone 1 (interior Jamaica) shows some linkage with the TNA (0.45). Zone 2 (eastern Jamaica) shows strong linkage with the gradient index (-0.46) and Caribbean low-level winds (-0.47) with Zone 3 (western Jamaica) showing some linkage with AMO (0.47) and TNA (0.43). Zone 4 (northern and southern Jamaica) showing strong linkage with the AMO (0.66) and NAO (-0.46) (Table 5).

Table 6. Concurrent and lagged correlations between bushfire frequency and climate indices for annual and seasonal periods calculated over 2001–2019. One year/season lags are calculated with climate leading (2000–2018). “-f” are the low pass filtered components. The correlations with LLW are over 2001–2018. Values in bold are significant at the 95% level.

	Annual		DJFM		AMJ		JA		SON	
	Lag-0	Lag-1	Lag-0	Lag-1	Lag-0	Lag-1	Lag-0	Lag-1	Lag-0	Lag-1
Rainfall	-0.05	0.16	-0.27	0.19	-0.08	0.12	-0.43	-0.48	-0.52	-0.38
Temp	0.01	-0.44	-0.45	0.57	0.04	-0.27	0.54	0.49	0.43	0.31
Rainfall-f	0.34	0.53	0.14	-0.34	-0.04	0.32	-0.64	-0.55	-0.58	-0.49
NAO	-0.15	-0.15	-0.45	-0.29	-0.02	0.03	-0.52	0.34	0.41	0.17
TNA	0.25	0.13	0.47	0.19	0.14	0.00	-0.59	-0.18	-0.41	-0.04
Nino3	0.10	-0.21	-0.34	-0.14	0.35	-0.23	0.57	-0.12	0.69	-0.13
TNA-Nino3	0.01	-0.22	0.45	0.19	-0.22	0.19	0.68	-0.03	0.72	0.09
TSA	-0.10	-0.03	0.08	-0.20	0.04	0.11	0.10	0.01	-0.27	-0.02
LLW	0.20	0.33	0.47	0.44	0.09	0.14	-0.66	-0.33	-0.54	-0.02
PDO-f	-0.30	-0.33	-0.50	-0.47	-0.16	-0.17	0.45	0.37	0.32	-0.20
AMO-f	0.63	0.47	0.39	0.35	0.50	0.30	0.22	0.22	0.20	0.18
NAO-f	-0.39	-0.41	-0.32	-0.47	-0.36	-0.27	0.08	0.25	0.27	0.16

Table 7. Correlations between annual bushfire frequency and some annual climate indices calculated over 2001–2019 for concurrent periods. “-f” are the low pass filtered components. Calculations with LLW and PDO are up to 2018 and 2017, respectively. Values in bold are significant at the 95% level.

	All Island	Zone 1	Zone 2	Zone 3	Zone 4
NAO	-0.15	-0.31	0.18	-0.32	0.05
TNA	0.25	0.45	-0.36	0.43	0.05
Nino	0.10	0.32	0.39	-0.01	-0.05
TNA-Nino3	0.01	-0.10	-0.46	0.17	0.06
TSA	-0.10	-0.01	-0.16	-0.01	-0.14
LLW	0.20	0.12	-0.47	0.34	0.16
PDO-f	-0.30	-0.05	0.36	-0.26	-0.34
AMO-f	0.63	0.33	0.17	0.47	0.66
NAO-f	-0.39	-0.06	0.11	-0.27	-0.46

Years of above normal fire variability are generally observed during El Niño events and below normal fire years are typically evident during La Niña years (See Table 8). Notably the super El Niño in 2015–2016 was observed alongside the 3rd highest fire anomalies recorded over 2001–2019. Composite analysis of Atlantic and Pacific SSTA shows a strong warming over the North middle to high latitude Atlantic with the warming extending over most of the North Atlantic during years of high bushfire frequency (Figure 9a). This is very similar to the characteristic AMO pattern [43,57]. During low fire years, a weakened warming is evident over much of the North Atlantic but with stronger warming over the Gulf of Mexico through the northern Caribbean and along a south-west to north east axis (Figure 9b). Notably oppositely signed SST anomalies over the Gulf of Mexico and the northern Caribbean emerge for the difference composite with Jamaica located in the transition zone (Figure 9c). This composite map is similar to the SST composite map obtained for high minus low years of the AMO [31]. The other dominant SST signal evident is the strong warming over the North Pacific through to the equatorial Pacific

during high years and below normal SSTAs in these regions in low years. The difference in North Pacific SSTAs is statistically significant. The warming pattern during high fire years shows some similarities to the PDO pattern. However, the PDO pattern shows negative SST anomalies over much of the north Pacific (with positive anomalies distributed in a horseshoe pattern from the equatorial Pacific and along the west coast of North America). See for example [58]. High fire years appear to have an ENSO like warming signal over the equatorial Pacific but a cool tongue (consistent with La Niña) was not observed for low fire years.

Table 8. Contingency table showing the occurrence of high and low fire years for Jamaica relative to El Niño and La Niña events identified using <http://www.bom.gov.au/climate/enso/enlist/> (accessed on 18 August 2020). Values in bold (underlined) are high (low) bushfire years used in the composite calculations.

Events	High Fire Years	Low Fire Years
El Niño	2006–2007, 2009–2010 , <u>2015–2016</u>	<u>2002–2003</u>
La Niña	2010–2012	<u>2001</u> , 2007–2008, 2008–2009
Neutral	2005	2004

Zonal winds during high years (Figure 9d) are positive over the Caribbean versus near zero anomalies over Jamaica and Cuba during low years (Figure 9e). The difference composite of zonal winds (Figure 9f) indicates positive values over the region and suggests a strengthening of low-level easterlies over the Caribbean during high fire years versus low years as represented in Figure 9d–f. Additionally, observed in the difference composite is an area of strong positive wind anomalies in the Caribbean low-level jet region (south of Jamaica) likely indicative of strengthened jet in this region during high years (positive values) versus low years (negative values) (Figure 9). Only small regions over the tropical Pacific and the United States are identified as statistically significant in the difference maps.

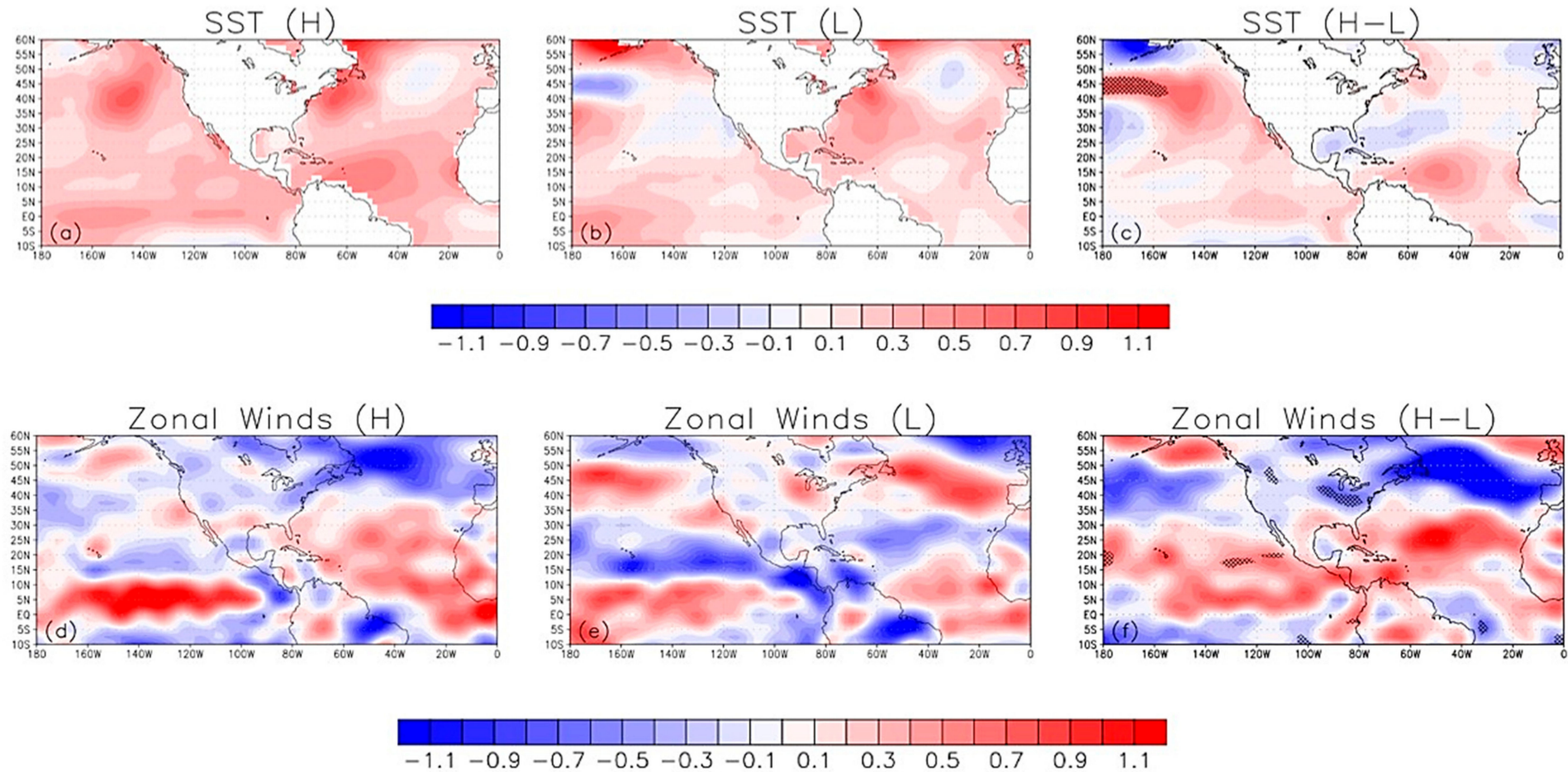


Figure 9. Composites of SSTA (K) and zonal wind anomalies (ms^{-1}) over the Pacific and Atlantic for high and low years of Jamaica fire frequency anomalies. (a–c) SSTA high, low and high minus low composite. (d–f) 925 mb zonal wind anomalies high, low and high minus low composite. Stippled areas show regions where composite differences are statistically significant at 95% confidence level.

4. Conclusions

In this study the variability of fire frequency over Jamaica is characterized using MODIS C6 data archive for 2001–2019. The data are found to be representative of fire occurrences for the island although values are below the land based JFB data by a factor of up to 30. Fires vary seasonally peaking in March and July. Positive trends in fire frequency are noted on average on annual and seasonal timescales except for December–March. The trend is strongest for July–August and represents 29% of the variability. Periodicities are significant for AMJ and SON where 5 year and 3.5-year cycles, respectively, are evident. Wavelet analysis on annual timescales by zones reveals a 6-year cycle over Zone 3 (western Jamaica). Southern Jamaica shows the greatest frequencies during December to March and particularly over Clarendon. Southern Jamaica is known for its climatological dryness.

Significant and fairly strong correlations were observed with rainfall for September–November (-0.52) and with temperature for July–August (0.54) with lagged correlations significant for JA temperatures. JA fire variability also showed some association with NAO (0.52), TNA (-0.59), Niño3 (0.57), TNA–Niño3 (0.68) and LLW (-0.66). Annual and DJFM and AMJ fire frequency exhibits variability similar to the Atlantic Multidecadal Oscillation (0.63) and some connection with the Pacific Decadal Oscillation (-0.50). The suggestion is that the influence of the large-scale climate features may be directly through wind patterns over the island and indirectly through interaction with rainfall.

Annual fire frequency activity explored by zone reveals correlations between Zone 1 (interior Jamaica) and TNA (0.45). Zone 2 (eastern Jamaica) shows some relationship with TNA–Niño3 (-0.46) and LLW (-0.47) with Zone 3 (western Jamaica) showing some association with AMO (0.47). Zone 4 (northern and southern Jamaica) showing strong linkage with the AMO (0.66) and NAO (-0.46). The significant correlations with filtered AMO, PDO and NAO suggest that some decadal variability is at work in Jamaica's fire frequency. The AMO has dominant periods at 20–30 years and 65–80 years [46]; the PDO at 15–25 and 50–70 years [59]; and NAO at 7–11 and 37–40 years [60,61]. Shorter term bushfire variability appears to be through the influence of the El Niño Southern Oscillation. Years of above normal fire variability are generally observed during El Niño events and below normal fire years are typically evident during La Niña years. It is useful to note that the positive correlations observed in relation to the AMO are obtained since bushfire frequency anomalies track the AMO but does so across positive and negative values while the AMO remains entirely positive.

Composite analysis of Atlantic and Pacific SSTA shows warming over the North middle to high latitude Atlantic consistent with the characteristic AMO pattern [44,57]. Oppositely signed SST anomalies over the Gulf of Mexico and the northern Caribbean also emerge for the difference composite with Jamaica located in the transition zone. This composite map is similar to the SST composite map obtained for high minus low years of the AMO [31]. The relationship observed between fire frequency anomalies and climate suggest that an early warning system for bushfires in Jamaica and perhaps the Caribbean should include monitoring some key climate variables temporally and spatially. These 'predictors' need not be the only triggers in the system but can serve to validate the expected bushfire anomalies given the large-scale synoptic patterns. The early warning mechanism being investigated for Jamaica will also look at fire potential using indices such as the Keetch Byram Drought Index (KBDI) and the Forest Fire Danger Index (FFDI). These indices incorporate rainfall, evapotranspiration, temperature and humidity. These indices will be instructive in determining how fire potential has been changing for Jamaica, assessing their correlation with large-scale modes such as ENSO, and determining whether the expectation that the potential increases in the future, i.e., toward the end of century, is a justifiable one. The final predictive framework will therefore allow for seasonal outlooks for bushfires as well as long term projections.

Notably the current fire observation data suggests that the JA bushfire trend is most significant in comparison to other seasons. Can we anticipate that the trend for this and other seasons will change in the future and what large-scale features will facilitate such

changes? This study demonstrates that even with bushfires there are different timescales at work, i.e., interannual, decadal and trend patterns and more work will be necessary to be able to attribute bushfire variability for Jamaica and the Caribbean. Expanding the countries under investigate will be useful in better understanding bushfire variability for the region. Furthermore, including total area burned and cause of fire in the data recorded as well as updating geocoded observed fire occurrences would be useful in advancing this research. Since the aim of this study is to advise planning and decision making it is also suggested that improved data collection and warning protocols be established to further develop bushfire management on the island.

Author Contributions: Conceptualization, C.S.C. and T.S.S.; methodology, C.S.C.; validation, C.S.C., T.S.S.; formal analysis, C.S.C. and C.A.D.; investigation, C.S.C.; resources, C.S.C.; data curation, C.S.C.; writing—original draft preparation, C.S.C.; writing—review and editing, T.S.S. and M.A.T.; visualization, C.S.C., C.A.D.; supervision, T.S.S. and M.A.T.; project administration, T.S.S. and M.A.T. All authors have read and agreed to the published version of the manuscript.

Funding: This research received no external funding.

Institutional Review Board Statement: Not applicable.

Informed Consent Statement: Not applicable.

Data Availability Statement: Please refer to suggested Data Availability Statements in section “MDPI Research Data Policies” at <https://psl.noaa.gov/data/correlation/tna.data> (accessed on 10 February 2020); <https://psl.noaa.gov/data/correlation/tsa.data> (accessed on 10 February 2020); <https://www.cpc.ncep.noaa.gov/data/indices/ersst5.nino.mth.81-10.ascii> (accessed on 10 February 2020); low-level winds: NCEP/NCAR Reanalysis $2.5^\circ \times 2.5^\circ$; <https://www.cpc.ncep.noaa.gov/data/teledoc/nao.shtml> (accessed on 10 February 2020); <https://www.esrl.noaa.gov/psd/data/timeseries/AMO/> (accessed on 25 March 2020); <http://research.jisao.washington.edu/pdo/PDO.latest.txt> (accessed on 25 March 2020); Source for MODIS dataset: <https://firms.modaps.eosdis.nasa.gov/download/> (accessed on 29 January 2020).

Acknowledgments: For their support one author (C.S.C.) would like to acknowledge the Jamaica Fire Brigade (JFB), especially Nicholas Ogilvie and Ricardo Young, as well as Kwesi Osborne. The author would also like to acknowledge the Meteorological Service Jamaica (MSJ), especially Jacqueline Spence-Hemmings and the data acquisition section. The authors (C.S.C., T.S.S., M.A.T. and C.A.D.) would like to acknowledge Jayaka Campbell from the Department of Physics, The University of the West Indies Mona.

Conflicts of Interest: Authors declare no conflict of interest.

References

1. The Jamaica Gleaner. Jamaica Fire Brigade Reporting an Increase in the Number of Bushfires. 18 April 2020. Available online: <https://www.jamaica-gleaner.com/article/news/20200418/jamaica-fire-brigade-reporting-increase-number-bush-fires> (accessed on 9 September 2020).
2. Countryman, C.M. *The Fire Environment Concept*; Pacific Southwest Forest and Range Experiment Station: Berkeley, CA, USA, 1972.
3. Johnson, E.A. *Fire and Vegetation Dynamics*; Cambridge University Press: Cambridge, UK, 1992.
4. Swetnam, T.W. Fire History and Climate Change in Giant Sequoia Groves. *Science* **1993**, *262*, 885–889. [[CrossRef](#)] [[PubMed](#)]
5. Weaver, P.; Gonzalez, K. (Eds.) *Wildland Fire Management and Restoration: Proceedings of the 12th Meeting of the Caribbean Foresters in Puerto Rico, 7–11 June 2004*; International Institute of Tropical Forestry, USDA Forest Service (IITF): Rio Piedras, Puerto Rico, 2005.
6. Robbins, A.M.J. *Global Forest Resources Assessment 2005—Report on Fires in the Caribbean and Mesoamerican Regions. Fire Management Working Paper 12*; FAO—Food and Agriculture Organization: Rome, Italy, 2006.
7. Robbins, A.M.J.; Eckelmann, C.-M.; Quinones, M. Forest Fires in the Insular Caribbean. *Ambio* **2008**, *37*, 528–534. [[CrossRef](#)] [[PubMed](#)]
8. Akpinar-Elci, M.; Coomansingh, K.; Blando, J.; Mark, L. Household bush burning practice and related respiratory symptoms in Grenada, the Caribbean. *J. Air Waste Manag. Assoc.* **2015**, *65*, 1148–1152. [[CrossRef](#)] [[PubMed](#)]
9. Litell, J.S.; Peterson, D.L.; Riley, K.L.; Liu, Y.; Luce, C.H. A review of the relationships between drought and forest fire in the United States. *Glob. Change Biol.* **2016**, *22*, 2353–2369. [[CrossRef](#)] [[PubMed](#)]
10. Harris, S.; Lucas, C. Understanding the variability of Australian fire weather between 1973 and 2017. *PLoS ONE* **2019**, *14*, e0222328. [[CrossRef](#)] [[PubMed](#)]

11. Parente, J.; Pereira, M.; Amraoui, M.; Tedim, F. Negligent and intentional fires in Portugal: Spatial distribution characterization. *Sci. Total Environ.* **2018**, *624*, 424–437. [[CrossRef](#)]
12. Wendler, G.; Conner, J.; Moore, B.; Shulski, M.; Stuefer, M. Climatology of Alaskan wildfires with special emphasis on the extreme year of 2004. *Theor. Appl. Climatol.* **2011**, *104*, 459–472. [[CrossRef](#)]
13. Turco, M.; Llasat, M.-C.; von Hardenberg, J.; Provenzale, A. Climate change impacts on wildfires in a Mediterranean environment. *Clim. Chang.* **2014**, *125*, 369–380. [[CrossRef](#)]
14. Trauernicht, C.; Pickett, E.; Giardina, C.P.; Litton, C.M.; Cordell, S.; Beavers, A. The Contemporary Scale and Context of Wildfire in Hawaii. *Pac. Sci.* **2015**, *69*, 427–444. [[CrossRef](#)]
15. Mouillot, F.; Field, C. Fire history and the global carbon budget: A $1^\circ \times 1^\circ$ fire history reconstruction for the 20th century. *Glob. Change Biol.* **2005**, *11*, 398–420. [[CrossRef](#)]
16. Koutsias, N.; Xanthopoulos, G.; Founda, D.; Xystrakis, F.; Nioti, F.; Pleniou, M.; Mallinis, G.; Arianoutsou, M. On the relationships between forest fires and weather conditions in Greece from long-term national observation (1894–2010). *Int. J. Wildland Fire* **2013**, *22*, 493–507. [[CrossRef](#)]
17. Pereira, M.; Malamud, B.; Trigo, R.; Alves, P. The history and characteristics of the 1980–2005 portuguese rural fire database. *Nat. Hazards Earth Syst. Sci.* **2011**, *11*, 3343–3358. [[CrossRef](#)]
18. Short, K. Sources and implications of bias and uncertainty in a century of US wildfire activity data. *Int. J. Wildland Fire* **2015**, *24*, 883–891. [[CrossRef](#)]
19. Turco, M.; Llasat, M.; Tudela, A.; Castro, X.; Provenzale, A. Decreasing fires in a Mediterranean region (1970–2010, NE Spain). *Nat. Hazards Earth Syst. Sci.* **2013**, *13*, 649–652. [[CrossRef](#)]
20. Stephenson, T.; Vincent, L.; Allen, T.; Van Meerbeek, C.; Mclean, N.; Peterson, T.; Taylor, M.A.; Aaron-Morrison, A.P.; Auguste, T.; Bernard, D.; et al. Changes in extreme temperature and precipitation in the Caribbean region. *Int. J. Climatol.* **2014**, *34*, 2957–2971. [[CrossRef](#)]
21. Peterson, T.C.; Taylor, M.A.; Demeritte, R.; Duncombe, D.L.; Burton, S.; Thompson, F.; Porter, A.; Mercedes, M.; Villegas, E.; Semexant Fils, R.; et al. Recent changes in climate extremes in the Caribbean region. *J. Geophys. Res. Space Phys.* **2002**, *107*, 4601. [[CrossRef](#)]
22. IPCC. *Managing the Risks of Extreme Events and Disasters to Advance Climate Change Adaptation*; Cambridge University Press: Cambridge, UK, 2012.
23. McSweeney, C.; Lizcano, G.; New, M.; Lu, X. The UNDP Climate Change Country Profiles: Improving the accessibility of observed and projected climate information for studies of climate change in developing countries. *Bull. Am. Meteorol. Soc.* **2010**, *91*, 157–166. [[CrossRef](#)]
24. Hall, T.C.; Sealy, A.M.; Stephenson, T.; Kusunoki, S.; Taylor, M.; Chen, A.; Kitoh, A. Future climate of the Caribbean from a super-high-resolution atmospheric general circulation model. *Theor. Appl. Climatol.* **2013**, *113*, 271–287. [[CrossRef](#)]
25. Mclean, N.; Stephenson, T.; Taylor, M.; Campbell, J. Characterization of Future Caribbean Rainfall and Temperature Extremes across Rainfall Zones. *Adv. Meteorol.* **2015**, *2015*, 1–18. [[CrossRef](#)]
26. Jones, P.D.; Harpham, C.; Harris, I.; Goodess, C.M.; Burton, A.; Centella-Artola, A.; Taylor, M.A.; Bezanilla-Morlot, A.; Campbell, J.D.; Stephenson, T.S.; et al. Long-term trends in precipitation and temperature across the Caribbean. *Int. J. Climatol.* **2016**, *36*, 3314–3333. [[CrossRef](#)]
27. Karmalkar, A.V.; Taylor, M.A.; Campbell, J.; Stephenson, T.; New, M.; Centella, A.; Benzanilla, A.; Charlery, J. A Review of Observed and Projected Changes in Climate for the Islands in the Caribbean. *Atmosfera* **2013**, *26*, 283–309. [[CrossRef](#)]
28. Campbell, J.D.; Taylor, M.A.; Stephenson, T.S.; Watson, R.A.; Whyte, F.S. Future climate of the Caribbean from a regional climate model. *Int. J. Climatol.* **2011**, *31*, 1866–1878. [[CrossRef](#)]
29. Taylor, M.A.; Clarke, L.A.; Centella, A.; Bezanilla, A.; Stephenson, T.S.; Jones, J.J.; Campbell, J.; Vichot, A.; Charlery, J. Future Caribbean Climates in a World of Rising Temperatures: The 1.5 vs 2 Dilemma. *J. Clim.* **2018**, *31*, 2907–2926. [[CrossRef](#)]
30. Walters, R.N. Examining Drought in Jamaica and the Caribbean. Unpublished Master’s thesis, University of the West Indies, Mona, Kingston, Jamaica, 2016.
31. Douglas, C.A.; Stephenson, T.S.; Taylor, M.A.; Brown, A.A.; Campbell, J.D.; Stennett-Brown, R.K.; Walters, R. Investigating decadal variability in Jamaica’s Rainfall: A Case Study for the Caribbean. *Theoret. Appl. Climatol.* **2020**. Submitted.
32. Chen, A.A.; Roy, A.; McTavish, J.; Taylor, M.; Marx, L. Using sea surface temperature anomalies to predict flood and drought conditions for the Caribbean. *COLA Rep.* **1997**, *49*, 24.
33. Taylor, M.A.; Enfield, D.B.; Chen, A.A. Influence of the tropical Atlantic versus the tropical Pacific on Caribbean rainfall. *J. Geophys. Res. Space Phys.* **2002**, *107*, 3127. [[CrossRef](#)]
34. Justice, C.; Gigliob, L.; Korontzia, S.; Owens, J.; Morissette, J.; Roy, D.; Descloitres, J.; Alleaume, S.; Petitcolin, F.; Kaufman, Y. The MODIS fire product. *Remote Sens. Environ.* **2002**, *83*, 244–262. [[CrossRef](#)]
35. Giglio, L.; Descloitres, J.; Justice, C.O.; Kaufman, Y.J. An Enhanced Contextual Fire Detection Algorithm for MODIS. *Remote Sens. Environ.* **2003**, *87*, 273–282. [[CrossRef](#)]
36. Enfield, D.B.; Mestas-Nunez, A.M.; Mayer, D.A.; Cid-Serrano, L. How ubiquitous is the dipole relationship in the tropical Atlantic Sea Surface Temperatures? *J. Geophys. Res. Ocean* **1999**, *104*, 7841–7848. [[CrossRef](#)]
37. Jury, M.; Malmgren, B.A.; Winter, A. Subregional precipitation climate of the caribbean and relationship with ENSo and NAO. *J. Geophys. Res. Space Phys.* **2007**, *112*. [[CrossRef](#)]

38. Gouirand, I.; Jury, M.R.; Sing, B. An analysis of low- and high-frequency summer climate variability around the caribbean antilles. *J. Clim.* **2012**, *25*, 3942–3952. [[CrossRef](#)]
39. Ren, H.; Zuo, J.; Deng, Y. Statistical predictability of Nino indices for two stages of ENSO. *Clim. Dyn.* **2019**, *52*, 5361–5382. [[CrossRef](#)]
40. Hossain, I.; Rasel, H.M.; Imteaz, M.A.; Mekanik, F. Long term seasonal rainfall forecasting using linear and non linear modelling approaches: A case study for Western Australia. *Meteorol. Atmos. Phys.* **2020**, *132*, 131–141. [[CrossRef](#)]
41. Whyte, F.S.; Taylor, M.A.; Stephenson, T.A.; Campbell, J.D. Features of the Caribbean Low level jet. *Int. J. Climatol.* **2008**, *28*, 119–128. [[CrossRef](#)]
42. Cook, K.; Vizy, E. Hydrodynamics of the Caribbean low-level jet and its relationship to precipitation. *J. Clim.* **2010**, *23*, 1477–1494. [[CrossRef](#)]
43. Chen, A.A.; Taylor, M.A. Investigating the link between early season Caribbean rainfall and the El Nino+1 year. *Int. J. Climatol.* **2002**, *22*, 87–106. [[CrossRef](#)]
44. Enfield, D.B.; Mestas-Nunez, A.M.; Trimble, P.J. The Atlantic multidecadal oscillation and its relation to rainfall and river flows in the continental U.S. *Geophys. Res. Lett.* **2001**, *28*, 2077–2080. [[CrossRef](#)]
45. Zhang, Y.; Wallace, J.; Battisti, D. Enso-like interdecadal variability. *J. Clim.* **1997**, *10*, 1004–1020. [[CrossRef](#)]
46. Frankcombe, L.; Dijkstra, H. Coherent multidecadal variability in North Atlantic sea level. *Geophys. Res. Lett.* **2009**. [[CrossRef](#)]
47. Zuur, A.; Ieno, E.N.; Walker, N.; Saveliev, A.A.; Smith, G.M. *Mixed Effects Models and Extensions in Ecology in R*; Springer Science & Business Media: New York, NY, USA, 2009.
48. Climate Studies Group, Mona (CSGM). *State of the Jamaican Climate 2015: Information for Resilience Building*; Produced for the Planning Institute of Jamaica (PIOJ): Kingston, Jamaica, 2017.
49. Mann, H. Non-parametric tests against trend. *Econometrica* **1945**, *13*, 245–259. [[CrossRef](#)]
50. Kendall, M. *Rank Correlation Methods*, 4th ed.; Charles Griffin: London, UK, 1975.
51. Yilmaz, A.G.; Hossain, I.; Perera, B.J.C. Effect of climate change and variability on extreme rainfall intensity–frequency–duration relationships: A case study of Melbourne. *Hydrol. Earth Syst. Sci.* **2014**, *18*, 4065–4076. [[CrossRef](#)]
52. Sen, P. Estimates of the Regression Coefficient based on Kendall’s Tau. *J. Am. Stat. Assoc.* **1968**, *63*, 1379–1389. [[CrossRef](#)]
53. Tan, X.; Gan, T.Y.; Shao, D. Wavelet analysis of precipitation extremes over Canadian ecoregions and teleconnections to large-scale climate anomalies. *J. Geophys. Res. Atmos.* **2016**, *121*, 14469–14486. [[CrossRef](#)]
54. Kuo, C.-C.; Gan, T.Y.; Yu, P.-S. Wavelet Analysis on the Variability, Teleconnectivity, and Predictability of the Seasonal Rainfall of Taiwan. *Mon. Weather Rev.* **2010**, *138*, 162–174. [[CrossRef](#)]
55. Huang, B.; Torne, P.; Banzon, V.; Boyer, T.; Chepurin, G.; Lawrimore, J.; Menne, M.; Smith, T.; Vose, R.; Zhang, H. Extended Reconstructed Sea Surface Temperature, Version 5 (ERSSTv5): Upgrades, Validations, and Intercomparisons. *J. Clim.* **2017**, *30*, 8179–8204. [[CrossRef](#)]
56. Dee, D.; Uppala, S.; Simmons, A.; Berrisford, P.; Poli, P.; Kobayashi, S.; Andrae, U.; Balmaseda, M.; Balsamo, G.; Bauer, P.; et al. The ERA-Interim reanalysis: Configuration and performance of the data assimilation system. *Q. J. R. Meteorol. Soc.* **2011**, *137*, 553–597. [[CrossRef](#)]
57. Curtis, S. The El Niño–Southern Oscillation and Global Precipitation. *Geogr. Compass* **2008**, *2*, 600–619. [[CrossRef](#)]
58. Mantua, N.; Hare, S.; Zhang, Y.; Wallace, J.; Francis, R. A pacific interdecadal climate oscillation with impacts on salmon production. *Bull. Am. Meteorol. Soc.* **1997**, *78*, 1069–1079. [[CrossRef](#)]
59. Mantua, N.J.; Hare, S.R. The Pacific Decadal Oscillation. *J. Oceanogr.* **2002**, *58*, 35–44. [[CrossRef](#)]
60. Hurrell, J.W. Decadal Trends in the North Atlantic Oscillation: Regional Temperatures and Precipitation. *Science* **1995**, *269*, 676–679. [[CrossRef](#)] [[PubMed](#)]
61. Markovic, D.; Koch, M. Wavelet and scaling analysis of monthly precipitation extremes in Germany in the 20th century: Interannual to interdecadal oscillations and the North Atlantic Oscillation influence. *Water Resour. Res.* **2005**, *41*. [[CrossRef](#)]